Damage diagnosis using time series analysis of vibration signals

2001 Smart Mater. Struct. 10 446

(http://iopscience.iop.org/0964-1726/10/3/304)

INSTITUTE OF PHYSICS PUBLISHING SMART MATERIALS AND STRUCTURES
Smart Mater. Struct. **10** (2001) 446–451 www.iop.org/Journals/sm PII: S0964-1726(01)22811-0

Damage diagnosis using time series analysis of vibration signals

Hoon Sohn[1] **and Charles R Farrar**[2]

Engineering Analysis Group (ESA-EA), M/S P946 Los Alamos National Laboratory, Los Alamos, NM 87545, USA

E-mail: sohn@lanl.gov and farrar@lanl.gov

Received 15 September 2000

Abstract

A novel time series analysis is presented to locate damage sources in a mechanical system, which is running in various operational environments. The source of damage is located by solely analyzing the acceleration time histories recorded from a structure of interest. First, a data normalization procedure is proposed. This procedure selects a reference signal that is 'closest' to a newly obtained signal from an ensemble of signals recorded when the structure is undamaged. Second, a two-stage prediction model (combining auto-regressive (AR) and auto-regressive with exogenous inputs (ARX) techniques) is constructed from the selected reference signal. Then, the residual error, which is the difference between the actual acceleration measurement for the new signal and the prediction obtained from the AR–ARX model developed from the reference signal, is defined as the damage-sensitive feature. This approach is based on the premise that if there were damage in the structure, the prediction model previously identified using the undamaged time history would not be able to reproduce the newly obtained time series measured from the damaged structure. Furthermore, the increase in residual errors would be maximized at the sensors instrumented near the actual damage locations. The applicability of this approach is demonstrated using acceleration time histories obtained from an eight degrees-of-freedom mass–spring system.

(Some figures in this article are in colour only in the electronic version; see `www.iop.org`)

1. Introduction

The process of implementing a damage detection strategy for aerospace, civil and mechanical engineering infrastructure is referred to as structural health monitoring (SHM). Here damage is defined as changes to the material and/or geometric properties of these systems, including changes to the boundary conditions and system connectivity, which adversely affect the system's performance. The SHM process involves the observation of a system over time using periodically sampled dynamic response measurements from an array of sensors, the extraction of damage-sensitive features from these measurements, and the statistical analysis of these features to determine the current state of system health. For long-term SHM, the output of this process is periodically updated information regarding the ability of the structure to perform its intended function in light of the inevitable aging and degradation resulting from operational environments. After extreme events, such as earthquakes or blast loading, SHM is used for rapid condition screening and aims to provide, in near real time, reliable information regarding the integrity of the structure. A recent collapse of a pedestrian walkway bridge in North Carolina, USA (http://www.cnn.com/2000/US/05/21/racetrack.collapse/index.html) has received a tremendous amount of media attention, emphasizing the importance of health and condition monitoring for such structures. Furthermore, major advances in sensor technology and wireless data transmission are making the development of such a monitoring system economically feasible.

Based on the work of Rytter (1993), the authors categorize the structural health monitoring process into five stages: (1) identification of damage presence in a structure, (2) localization of damage, (3) identification of the damage type, (4) quantification of damage severity, and (5) prediction of the remaining service life of the structure. Doebling *et al*

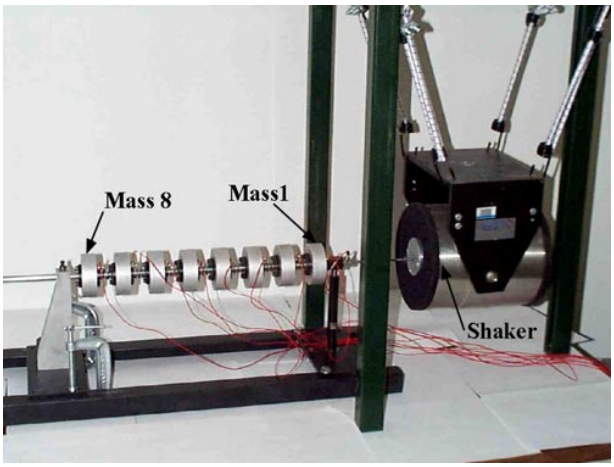

Figure 1. An 8 DOF system attached to a shaker with accelerometers mounted on each mass.

(1998) present a recent thorough review of the vibration-based damage identification methods. While the references cited in this review propose many different methods for identifying and localizing damage from vibration response measurements, the majority of the cited references rely on finite element modeling processes and/or linear modal properties for damage diagnosis. For practical applications these methods have not been shown to be effective in detecting damage at an early state. To avoid the shortcomings of the methods summarized in this review, the authors have been tackling the damage detection problems based exclusively on statistical analysis of time series.

The authors pose the SHM process in the context of a statistical pattern recognition paradigm. This paradigm can be described as a four-part process: (1) operational evaluation, (2) data acquisition and cleansing, (3) feature extraction and data reduction, and (4) statistical model development. In particular, this paper focuses on parts 3 and 4 of the process. A more detailed discussion of the statistical pattern recognition paradigm can be found in Farrar *et al* (2000). It should be noted that neither sophisticated finite element models nor the traditional modal parameters are employed in the implementation of the proposed paradigm because they often require labor intensive tuning and result in significant uncertainties caused by user interaction and modeling errors. The approach presented here is solely based on signal analysis of the measured vibration data, making this approach very attractive for the development of an automated health monitoring system. This signal-only-based paradigm has been applied to the damage identification problem by the authors (Sohn *et al* 2000, Fugate *et al* 2001). In this paper, the paradigm is extended to the second level damage diagnosis, *damage localization problems*. The applicability of the proposed approach is investigated using a simple eight degrees of freedom (8 DOF) mass–spring system tested in a laboratory environment.

2. Test structure

An 8 DOF system has been designed and constructed to study the effectiveness of the proposed localization procedure. The system is formed of eight translating masses connected by springs. The system employed in this study is shown in figure 1. Each mass is an aluminum disk 25.4 mm thick and 76.2 mm in diameter with a central hole. The hole is lined with a Teflon bush. There are small steel collars on each end of the disks (figure 2). The masses all slide on a highly polished steel rod that supports the masses and constrains them to translate only along the rod. The masses are fastened together with coil springs epoxied to the collars that are, in turn, bolted to the masses.

Table 1. Specifications for data acquisition.

Time step	0.001 953 s
Sampling rate	512 Hz
Time period	8 s
Frequency resolution	0.125 Hz
Number of data points	4096
Filtering	Uniform window
Nyquist frequency	256 Hz

The DOF, springs and masses are numbered from the right-hand end of the system, where the excitation is applied, to the left-hand end, as shown in figure 1. The nominal value of mass 1 (m1) is 559.3 g. Again, this mass is located at the right-hand end where the shaker is attached. m1 is greater than the others because of the hardware needed to attach the shaker. All the other masses (m2–m8) are 419.4 g. The spring constant for all the springs is 56.7 kN m^{-1} for the initial condition. Damping in the system is caused primarily by Coulomb friction. Every effort is made to minimize the friction through careful alignment of the masses and springs. A common commercial lubricant is applied between the Teflon bushes and the support rod.

Measurements made during damage identification tests were the excitation force applied to m1 and the acceleration response of all masses. Random excitation was accomplished with a 215 N peak force electro-dynamic shaker (figure 1). The root mean square (RMS) amplitude level of the input was varied from 3 to 7 V. A Hewlett-Packard 3566A system was employed for data acquisition. A laptop computer was used for data storage and for controlling the data acquisition system. The force transducer used had a nominal sensitivity of 22.48 mV N^{-1}, and the accelerometers had a nominal sensitivity of 10 mV g^{-1}. The specifications for the data acquisition are summarized in table 1.

The undamaged configuration of the system is the state for which all springs are identical and have a linear spring constant. Nonlinear damage is defined as the occurrence of impact between two adjacent masses. Damage is simulated by placing a bumper between two adjacent masses so that the movement of one mass is limited relative to the other mass. Figure 2 shows the hardware used to simulate nonlinear damage. When one end of a bumper, which is placed on one mass, hits the other mass, impact occurs. This impact simulates damage caused by the impact from the closing of a crack during vibration. The degree of damage can be controlled by changing the amount of relative motion permitted before contact, and changing the hardness of the bumpers on the impactors. For all damage cases presented, the initial clearance is set to zero.

3. Analysis procedure

When one attempts to apply the statistical pattern recognition paradigm for SHM to data from real-world structures, it quickly becomes apparent that the ability to normalize data in an effort to account for operational and environmental variability is a key implementation issue when addressing parts 2–4 of this paradigm. For SHM strategies that rely on vibration response measurements, the ability to normalize the measured data with respect to varying operational and environmental conditions is essential if one is to avoid false-positive indication of damage. Examples of common normalization procedures include normalizing the response measurements by the measured inputs as is commonly done when extracting modal parameters. When environmental cycles influence the measured data, a temporal normalization scheme may be employed. These strategies for SHM data normalization fall into two general classes: (1) those employed when measures of the varying environmental and operational parameters are available and (2) those employed when such measures are not available. A primary focus of this study is to develop a data normalization procedure that can be employed for case 2 when measures of the varying environmental and operational conditions are not available.

The data normalization procedure begins by assuming that a 'pool' of signals is acquired from various unknown operational and environmental conditions, but from a known structural condition of the system. The ability of this procedure to normalize the data will be directly dependent on this pool being representative of data measured in as many varying environmental and operational conditions as possible. In the example reported herein, multiple time series are recorded from the undamaged structure (the known structural condition) at different input force levels (various operational conditions). The collection of these time series is called 'the reference database' in this study.

A two-stage prediction model, combining an auto-regressive (AR) model and an auto-regressive model with exogenous inputs (ARX), is employed to compute the damage-sensitive feature. In this case the damage-sensitive feature is the residual error between the prediction model and measured time series.

First, all time signals are standardized prior to fitting an AR model such that

$$\hat{x} = \frac{x - \mu_x}{\sigma_x} \tag{1}$$

where $\hat{x}$ is the standardized signal and μ_x and σ_x are the mean and standard deviation of x, respectively. This standardization procedure is applied to all signals employed in this study. (However, for simplicity, x is used to denote $\hat{x}$ hereafter.)

For each time series $x(t)$ in the reference database, an AR model with p AR terms is constructed. An AR(p) model can be written as (Box *et al* 1994)

$$x(t) = \sum_{j=1}^{p} \phi_{xj} x(t-j) + e_x(t). \tag{2}$$

This step is repeated for all signals in the reference database. The AR order is set to be 30 based on a partial auto-correlation analysis described in Box *et al* (1994).

Employing a new segment $y(t)$ obtained from an unknown structural condition of the system, repeat the previous step. Here the new segment $y(t)$ has the same length as the signal $x(t)$:

$$y(t) = \sum_{j=1}^{p} \phi_{yj} y(t-j) + e_y(t). \tag{3}$$

Then, the signal segment $x(t)$ 'closest' to the new signal block $y(t)$ is defined as the one that minimizes the following difference of AR coefficients:

$$\text{Difference} = \sum_{j=1}^{p} (\phi_{xj} - \phi_{yj})^2. \tag{4}$$

This 'data normalization' is a procedure to select the previously recorded time signal from the reference database, which is recorded under operational and/or environmental conditions closest to those of the newly obtained signal. If the new signal block is obtained from an operational condition close to one of the reference signal segments and there has been no structural deterioration or damage to the system, the dynamic characteristics (in this case, the AR coefficients) of the new signal should be similar or 'closest' to those of the reference signal based on the Euclidean distance measure in equation (4).

When a time prediction model is constructed from the selected reference signal, this prediction model should be able to appropriately predict the new signal if the new signal is 'close' to the reference signal. On the other hand, if the new signal was recorded under a structural condition different from the conditions where reference signals were obtained, the prediction model estimated from even the 'closest' signal in the reference database would not reproduce the new signal well.

For the construction of a two-stage prediction model proposed in this study, it is assumed that the error between the measurement and the prediction obtained by the AR model ($e_x(t)$ in equation (2)) is mainly caused by the unknown external input. Based on this assumption, an ARX model is employed to reconstruct the input/output relationship between $e_x(t)$ and $x(t)$:

$$x(t) = \sum_{i=1}^{a} \alpha_i x(t-i) + \sum_{j=1}^{b} \beta_j e_x(t-j) + \varepsilon_x(t) \tag{5}$$

where $\varepsilon_x(t)$ is the residual error after fitting the ARX(a, b) model to the $e_x(t)$ and $x(t)$ pair. Our feature for damage diagnosis will later be related to this quantity, $\varepsilon_x(t)$. Note that this AR–ARX modeling is similar to a linear approximation method of an auto-regressive moving-average (ARMA) model presented in Ljung (1987) and references therein. Ljung (1987) suggested keeping the sum of a and b smaller than p ($a + b \leqslant p$). ARX(5, 5) is used in this example. Although the a and b values of the ARX model are set rather arbitrarily, similar results are obtained for different combinations of a and b values as long as the sum of a and b is kept smaller than p.

Next, it is investigated how well this ARX(a, b) model estimated in equation (5) reproduces the input/output relationship of $e_y(t)$ and $y(t)$:

$$\varepsilon_y(t) = y(t) - \sum_{i=1}^{a} \alpha_i y(t-i) - \sum_{j=0}^{b} \beta_j e_y(t-j) \tag{6}$$

where $e_y(t)$ is considered to be an approximation of the system input estimated from equation (3). Again, note that the α_i and β_j coefficients are associated with $x(t)$ and obtained from equation (5). Therefore, if the ARX model obtained from the reference signal block pair $x(t)$ and $e_x(t)$ were not a good representation of the newly obtained signal segment pair $y(t)$ and $e_y(t)$, there would be a significant change in the standard deviation of the residual error, $\varepsilon_y(t)$, compared to that of $\varepsilon_x(t)$. In particular, the standard deviation ratio of the residual errors, $\sigma(\varepsilon_y)/\sigma(\varepsilon_x)$, is expected to reach its maximum value near the actual damage sources revealing the location of damage. Therefore, the standard deviation ratio of the 'similar' signals, $\sigma(\varepsilon_y)/\sigma(\varepsilon_x)$, is defined as the damage-sensitive feature and the increase of this ratio is monitored to detect system anomalies.

First, a statistical model is developed based on the normality assumption of underlying distributions $\sigma(\varepsilon_y)$ and $\sigma(\varepsilon_x)$. The primary objective is to test the null hypothesis, H_0: $\sigma^2(\varepsilon_x) = \sigma^2(\varepsilon_y)$, against the one-sided alternative H_1: $\sigma^2(\varepsilon_x) < \sigma^2(\varepsilon_y)$. Here $\sigma^2(\varepsilon_x)$ and $\sigma^2(\varepsilon_y)$ are the variances of ε_x and ε_y, respectively. It can be shown that the following sample variance ratio

$$F = \frac{\sigma^2(\varepsilon_y)}{\sigma^2(\varepsilon_x)} \tag{7}$$

has an F-distribution with $n_y - 1$ and $n_x - 1$ DOF under the null hypothesis H_0 (Miller 1997). n_x and n_y are the numbers of samples of $\varepsilon_x(t)$ and $\varepsilon_y(t)$, respectively. The null hypothesis H_0 is rejected when the F-statistic in equation (7) exceeds the upper $100 \times \alpha$ percentile of the F-distribution:

$$\frac{\sigma^2(\varepsilon_y)}{\sigma^2(\varepsilon_x)} > F^{\alpha}_{n_y-1,n_x-1}. \tag{8}$$

When the sample distribution departs from the normal distribution, the actual significance level in equation (8) can be considerably different from the normally stated level. For a heavy-tailed distribution the probability of rejection under H_0 greatly exceeds α, and for a short-tailed distribution the probability is considerably less than α.

Based on permutation theory, Box and Andersen (1955) modified equation (8) to safely use it in more general applications without a normality assumption. In the Box–Andersen test, the same F-statistic is computed. This statistic is, however, compared with a different critical point of the F-distribution with $n_y^* - 1$ and $n_x^* - 1$ degrees of freedom:

$$\frac{\sigma^2(\varepsilon_y)}{\sigma^2(\varepsilon_x)} > F^{\alpha}_{n_y^*-1,n_x^*-1} \tag{9}$$

where

$$n_x^* - 1 = d(n_x - 1) \qquad n_y^* - 1 = d(n_y - 1)$$

$$d = [1 + \tfrac{1}{2}(b - 3)]^{-1} \tag{10}$$

and

$$b = \frac{(n_x + n_y)(\sum \varepsilon_x^4(t) + \sum \varepsilon_y^4(t))}{(\sum \varepsilon_x^2(t) + \sum \varepsilon_y^2(t))^2}. \tag{11}$$

Here it is assumed that $\varepsilon_x(t)$ and $\varepsilon_y(t)$ are zero-mean processes. Otherwise, their mean values should be subtracted before the computation of the moments in equation (11). Note that when $\varepsilon_x(t)$ and $\varepsilon_y(t)$ are normal distributions with the same variance, equation (9) becomes identical to equation (8) since $b = 3$ and $d = 1$.

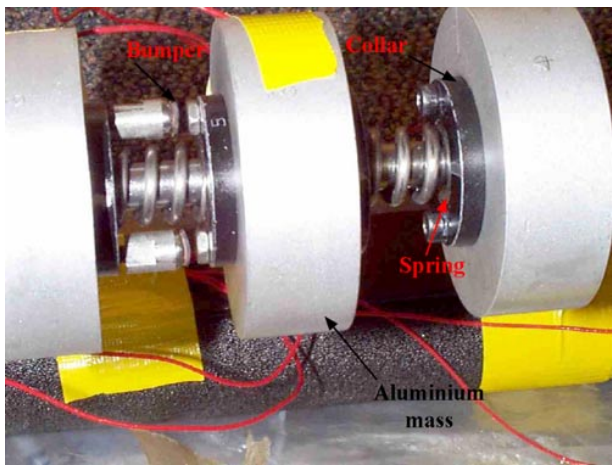

Figure 2. A typical bumper used to simulate nonlinear damage.

Various studies based on Monte Carlo simulation (Miller 1997 and references therein) have demonstrated that this Box–Andersen test maintains reasonably correct significance levels under the null hypothesis for a variety of heavy- and short-tailed distributions. This method also has been shown to be superior to most other competitive tests. This modified hypothesis test is employed to check if the new signal has significantly changed from the closest signal selected from the reference database.

4. Laboratory test result: an 8-DOF mass–spring system

For the localization study of nonlinear damage, three different damage scenarios are studied varying damage locations and input force levels. To simulate nonlinear damage, a bumper is placed between two masses as shown in figure 2. This bumper is installed between m1–m2, m5–m6, and m7–m8 for damage cases 1, 2, and 3, respectively. For each damage case, five sets of time histories are recorded at an individual input level and the input force varies from 3 V to 4, 5, 6, and 7 V (except damage case 3, where the input voltage varies from 4 to 7 V). Therefore, a total of 25, 25, and 20 time series are recorded for damage cases 1, 2, and 3, respectively. For the undamaged case, 15 sets of time histories are recorded at an individual input level, producing a total of 75 time series. To construct the reference database, which represents various operation conditions of the system, nine sets of time series were obtained from an individual input level and the input level again varies from 3 to 7 V. Therefore, 45 time series out of 75 time histories are used to construct the reference database. Table 2 summarizes the time series studied in this example.

Table 3 presents the standard deviation ratio, $\sigma(\varepsilon_y)/\sigma(\varepsilon_x)$, for each DOF and all damage cases. The $\sigma(\varepsilon_y)/\sigma(\varepsilon_x)$ values shown in table 3 are the mean values of 75, 25, 25, and 20 sample standard deviation ratios for damage cases 0, 1, 2, and 3, respectively. If a bumper were introduced at m1, the largest increase in the residual error standard deviation would be expected at the nearest measurement point, m1. However, as

Table 2. List of time series employed in this study.

Case	Description	Input level (V)	Data sets per input	Total data sets
0	No bumper	3, 4, 5, 6, 7	15	75
1	Bumper between m1–m2	3, 4, 5, 6, 7	5	25
2	Bumper between m5–m6	3, 4, 5, 6, 7	5	25
3	Bumper between m7–m8	4, 5, 6, 7	5	20

Table 3. $\sigma(\varepsilon_y)/\sigma(\varepsilon_x)$ ratio for various damage cases. Note that 15 data sets are recorded at each input level for the undamaged case, and 5 data sets are measured at an individual input level for all damage cases. The $\sigma(\varepsilon_y)/\sigma(\varepsilon_x)$ ratios presented are the average values of all input levels, i.e. the averages of 75, 25, 25, and 20 individual $\sigma(\varepsilon_y)/\sigma(\varepsilon_x)$ values measured under different input levels are presented for damage cases 0, 1, 2 and 3, respectively.

	DOF							
Bumper location	m1	m2	m3	m4	m5	m6	m7	m8
No bumper	1.0010	0.9965	1.0000	0.9992	1.0087	0.9988	1.0072	1.0009
Between m1–m2	1.0225	3.1101	1.2500	1.0628	1.1067	1.0425	1.0065	1.0751
Between m5–m6	0.9982	1.0345	0.9988	1.0478	2.6740	1.2564	1.2415	1.1558
Between m7–m8	1.0041	1.0106	1.0196	1.0575	1.1085	1.2572	2.4658	2.7610

shown in table 3, no significant increase in $\sigma(\varepsilon_y)/\sigma(\varepsilon_x)$ was observed at m1. Instead, the $\sigma(\varepsilon_y)/\sigma(\varepsilon_x)$ value in the next adjacent measurement point, m2, was significantly increased to 3.1101 on average. It is speculated that because m1 is rigidly connected to the shaker by a rod, the response at this point is masked by the direct influence of the random input. When the bumper was placed at m5, the average $\sigma(\varepsilon_y)/\sigma(\varepsilon_x)$ value in m5 increased to 2.6740, marking the largest increase among all masses (see the fourth row of table 3). A similar result is observed when the bumper is placed at m7 (see the fifth row of table 3). Here a simple chart of the $\sigma(\varepsilon_y)/\sigma(\varepsilon_x)$ values with respect to measurement points seems to reveal the approximate locations of nonlinear damage.

Next the hypothesis test presented in equation (8) is conducted for all test data, and summarized in table 4. The entries in table 4 show the rejection number of the null hypothesis H_0: $\sigma^2(\varepsilon_x) = \sigma^2(\varepsilon_y)$ out of all hypothesis tests. For example, when the hypothesis test is conducted on 75 time series data sets obtained from the undamaged case, the null hypothesis is rejected twice at m2 (2/75, as shown under the 'm2' column and the 'no bumper' row in table 4). In general, the number of rejections is minimum when no bumper is installed in the system, but a large number of rejections are observed for the subsequent damage cases. In particular, the number of rejections reaches its peak value near the actual location.

Table 5 reveals that the amplification of the input force introduces amplitude-dependent nonlinearity, causing the increase in $\sigma(\varepsilon_y)/\sigma(\varepsilon_x)$. For example, when the bumper is placed between m1 and m2, the $\sigma(\varepsilon_y)/\sigma(\varepsilon_x)$ value at m2 gradually increases in accordance with the input level. However, the input amplification alone did not cause any noticeable increase in the standard deviation ratio without the installation of a bumper. That is, the variation of the input force level did not produce false-positive indication of damage by employing an appropriate normalization procedure proposed in this paper.

5. Summary and discussions

This paper presents a procedure for damage detection and localization within a mechanical system solely based on the time series analysis of vibration signals. The standard deviation of the residual errors, which is the difference between the actual measurement and the prediction derived from a combination of the AR and ARX models, is used as our damage-sensitive feature to locate damage. The premise of this approach is that the residual error associated with the combined AR and ARX models developed from data obtained when the structure is undamaged will significantly increase when this model is applied to data obtained from a damaged system. Also, a larger increase in the standard deviation of the residual error is expected to be observed near the actual damage regions.

To minimize false positive warning of damage, a unique data normalization procedure is proposed to differentiate the effects of various environmental and/or operation conditions on the system dynamics from those caused by damage. This normalization procedure does not assume that measures of the environmental or operational conditions are available. However, it does assume that the reference database obtained when the structure is undamaged spans the various environmental and operational conditions that might influence the dynamics response of the system.

The proposed damage detection and localization approach has several desirable attributes. First, a single-dimensional data feature is used to both detect and locate damage. The use of a single-dimensional data feature enhances the ability to quantify the statistical variability in this feature as is discussed in most texts on statistical pattern recognition, for example see Bishop (1995). Also, the damage detection is conducted in an unsupervised learning mode. That is, data from the damaged structure are not needed to develop a classification model. Instead, the proposed procedure can be thought of as a form of outlier detection. The ability to perform the damage detection in an unsupervised learning mode is very important because data from damaged structures are typically not available for most real-world structures.

Finally, the approach presented herein is very attractive for the development of an automated continuous monitoring

Table 4. Results of hypothesis tests (H_0: $\sigma^2(\varepsilon_x) = \sigma^2(\varepsilon_y)$ and H_1: $\sigma^2(\varepsilon_x) < \sigma^2(\varepsilon_y)$. This table shows the rejecting numbers of the null hypothesis. For example, 2/75 means that the null hypothesis is rejected two times out of all tested 75 hypothesis tests. The Box–Andersen test is conducted with $\alpha = 0.01$.

	DOF							
Bumper location	m1	m2	m3	m4	m5	m6	m7	m8
No bumper	0/75	2/75	0/75	2/75	4/75	3/75	7/75	2/75
Between m1–m2	2/25	25/25	25/25	13/25	20/25	12/25	5/25	15/25
Between m5–m6	0/25	11/25	2/25	9/25	25/25	25/25	22/25	21/25
Between m7–m8	0/20	6/20	3/20	8/20	15/20	18/20	20/20	20/20

Table 5. Variation of $\sigma(\varepsilon_y)/\sigma(\varepsilon_x)$ ratios according to input voltage levels. Note that five data sets are recorded at each input level. The $\sigma(\varepsilon_y)/\sigma(\varepsilon_x)$ ratio presented is the average value of the five data sets. A bumper is placed between m1 and m2 during the acquisition of all the time series used in this analysis.

	DOF							
Input force level (V)	m1	m2	m3	m4	m5	m6	m7	m8
3	1.0128	2.6354	1.2283	1.0357	1.1781	1.0624	1.0075	0.9996
4	1.0160	2.9535	1.1135	1.0583	1.0523	1.0026	0.9931	1.1250
5	1.0338	3.2642	1.1902	1.0266	1.0891	1.0752	0.9894	1.1173
6	1.0268	3.2185	1.2528	1.0824	1.0786	1.0474	1.0190	1.0637
7	1.0233	3.4791	1.4652	1.1110	1.1353	1.0252	1.0235	1.0702

system because of its simplicity and because it requires minimal interaction with users. Furthermore, because damage diagnosis is conducted independently at an individual sensor level, time synchronization among the multiple sensors is not necessary. This characteristic makes it an attractive candidate for data interrogation with a wireless sensing system. However, it should be pointed out that the procedure developed has only been verified on relatively simple laboratory test specimens. To verify that the proposed method is truly robust, it will be necessary to examine many time records corresponding to a wide range of operational and environmental cases, a wide range of damaged and undamaged structures, as well as different damage scenarios. Herein lies one of the fundamental challenges for the further development and adaptation of any SHM scheme. The cost associated with such proof-of-concept testing is extremely high, and the access to infrastructure that can be damaged in a realistic manner is very limited.

Acknowledgments

All members of the Los Alamos Structural Health Monitoring Team contributed to this the study reported herein. The team members include George Papcum, Michael L Fugate and Donald R Hush from the Computing, Information, and Communications Group, Norm F Hunter from the Measurement Technology group, and Scott Doebling from the Engineering Analysis Group. Funding for this investigation came primarily through the Los Alamos National Laboratory's Director Funded Postdoctoral Fellowship Program. The authors also would like to thank Dr Winston Rhee for his contribution to the experimental portion of this paper.

References

Bishop C M 1995 *Neural Networks for Pattern Recognition* (Oxford: Oxford University Press)

Box G E P and Andersen S L 1995 Permutation theory in the derivation of robust criteria and the study of departures from assumption *J. R. Statist. Soc.* B **17** 1–26

Box G E P, Jenkins G M and Reinsel G C 1994 *Time Series Analysis: Forecasting and Control* 3rd edn (Englewood Cliffs, NJ: Prentice-Hall)

Doebling S W, Farrar C R, Prime M B and Shevitz D W 1998 A review of damage identification methods that examine changes in dynamic properties *Shock Vibr. Dig.* **30** 95–105

Farrar C R, Duffey T A, Doebling S W and Nix D A 2000 A statistical pattern recognition paradigm for vibration-based structural health monitoring *Proc. 2nd Int. Workshop on Structural Health Monitoring (Stanford, CA, September 8–10, 2000)* pp 764–73

Fugate M L, Sohn H and Farrar C R 2001 Vibration-based damage detection using statistical process control *Mech. Syst. Signal Proc.* at press

Ljung L 1987 *System Identification: Theory for the User* (Englewood Cliffs, NJ: Prentice-Hall)

Miller R G 1997 *Beyond ANOVA: Basics of Applied Statistics* (New York: Chapman and Hall)

Rytter A 1993 Vibration based inspection of civil engineering structures *PhD Dissertation* Department of Building Technology and Structural Engineering, Aalborg University, Denmark

Sohn H, Czarnecki J J and Farrar C R 2000 Structural health monitoring using statistical process control *J. Eng. Mech., ASCE* at press